Food and Chemical Toxicology 129 (2019) 125–137

Contents lists available at ScienceDirect

Food and Chemical Toxicology

journal homepage: www.elsevier.com/locate/foodchemtox

Protective effects of extract of *Cleistocalyx operculatus* flower buds and its isolated major constituent against LPS-induced endotoxic shock by activating the Nrf2/HO-1 pathway

Phi-Long Tran[a], Okwha Kim[a], Huynh Nguyen Khanh Tran[b], Manh Hung Tran[c], Byung-Sun Min[b], Cheol Hwangbo[d], Jeong-Hyung Lee[a,*]

[a] Department of Biochemistry, College of Natural Sciences, Kangwon National University, Chuncheon, Gangwon-Do, 24414, Republic of Korea
[b] College of Pharmacy, Catholic University of Daegu, Gyeongbuk, 38430, Republic of Korea
[c] Medicinal Chemistry Division, Faculty of Chemistry, University of Science, Vietnam National University, 227 Nguyen Van Cu, District 5, Ho Chi Minh City, 748000, Viet Nam
[d] Division of Applied Life Science (BK21 Plus), PMBBRC, Division of Life Science, College of Natural Sciences, Gyeongsang National University, Jinju, 52828, Republic of Korea

ARTICLE INFO

Keywords:
Cleistocalyx operculatus flower buds
Septic shock
Anti-inflammation
Nrf2
Heme oxygenase-1

ABSTRACT

The flower buds of *Cleistocalyx operculatus* are used as an important ingredient in herbal tea and herbal products in several tropical countries. However, their protective effects and underlying mechanisms on lipopolysaccharide (LPS)-induced endotoxic shock remain unclear. The aim of this study was to investigate the anti-inflammatory effects of ethanol extract of *C. operculatus* flower buds (ECO) and its major constituent 2′,4′-dihydroxy-6′-methoxy-3′,5′-dimethylchalcone (DMC) in macrophages and in an experimental LPS-induced sepsis mouse model. ECO inhibited the LPS-induced production and expression of pro-inflammatory mediators in macrophages. In an endotoxic shock mouse model, the oral administration of ECO rescued LPS-induced mortality, and attenuated LPS-induced increases in the serum levels of pro-inflammatory mediators, and damage of the lung and liver tissues. ECO increased the nuclear translocation of the nuclear factor erythroid 2-related factor 2 (Nrf2), as well as the expression of Nrf2 target genes, including heme oxygenase-1 (HO-1), in macrophages. Similar to the effects of ECO, DMC also inhibited the LPS-induced inflammatory response in macrophages and endotoxic shock in mice, and activated the Nrf2/HO-1 pathway. In conclusion, our findings suggested that ECO and its major constituent, DMC, attenuated LPS-induced endotoxic shock by activating the Nrf2/HO-1 pathway.

1. Introduction

Inflammation is an adaptive response that is triggered by invading microbes or physical injuries (Medzhitov, 2008). Macrophages mediate most of the cellular and molecular pathophysiology of inflammation by producing various pro-inflammatory mediators, including tumor necrosis factor-α (TNF-α), interleukin (IL)-1β, IL-6, and nitric oxide (NO) (Laskin et al., 2011; Murray, 2017). Unregulated production of these pro-inflammatory mediators has been implicated in a wide range of diseases, including rheumatoid arthritis, inflammatory bowel disease, sepsis, and asthma (Benoit et al., 2008; Tabas and Glass, 2013).

Lipopolysaccharide (LPS) is a bacterial endotoxin that triggers inflammatory response via toll-like receptor-4 (TLR4) (Akira and Takeda, 2004). Binding of LPS to TLR-4/myeloid differentiating factor 2 (MD-2) complex leads to activation of a unique set of intracellular signaling pathways, the myeloid differentiation factor-88 (MyD88)-dependent pathway and the TIR domain-containing adaptor inducing interferon-β (TRIF)-dependent pathway (Aderem and Ulevitch, 2000; Zhang and Ghosh, 2001). The MyD88-dependent pathway mediates the activation of IκB kinases, extracellular signal-related kinase (ERK)-1/2, c-Jun NH_2-terminal kinase (JNK), and p38 mitogen-activated protein kinases (MAPKs), leading to activation of transcription factors, such as the nuclear factor-κB (NF-κB) and AP-1 (Aderem and Ulevitch, 2000; Zhang and Ghosh, 2001). The nuclear factor erythroid 2-related factor 2 (Nrf2) is a member of the basic-leucine zipper transcription factor family that contributes to anti-inflammatory processes (Moi et al., 1994; Jaramillo and Zhang, 2013). Nrf2 controls the expression of a number of antioxidant and cyto-protective genes, such as heme oxygenase-1 (HO-1), NAD(P)H:quinone oxidoreductase 1 (NQO1), and γ-glutamyl cysteine synthetase catalytic subunit (GCLC) (Moi et al., 1994; Jaramillo and

* Corresponding author. Tel.: +82 33 250 8519; fax: +82 33 259 5664.
E-mail address: jhlee36@kangwon.ac.kr (J.-H. Lee).

https://doi.org/10.1016/j.fct.2019.04.035
Received 5 December 2018; Received in revised form 11 April 2019; Accepted 19 April 2019
Available online 25 April 2019
0278-6915/

Zhang, 2013). In macrophages, Nrf2 also suppresses the inflammatory response by blocking the pro-inflammatory cytokine transcription (Bryan et al., 2013). Among the genes that are regulated by Nrf2 activation, HO-1 is considered to be the major anti-inflammatory and cytoprotective enzyme (Paine et al., 2010; Abraham and Kappas, 2008; Motterlini and Foresti, 2014). Extensive studies have suggested that the Nrf2 activators have a protective effect in inflammatory diseases, including sepsis (Ahmed et al., 2017). Therefore, targeting the Nrf2 pathway with phytochemicals may represent a promising strategy for the prevention or treatment of inflammatory diseases (Motterlini and Foresti, 2014; Ahmed et al., 2017).

Cleistocalyx operculatus (Roxb.) Merr. and Perry (Myrtaceae) is a well-known edible plant, and is widely distributed in Southeast Asia, including Vietnam. Its dried flower buds have been used as an important ingredient of herbal tea for thousands of years (Loi, 1986). The flower buds of *C. operculatus* are a rich source of bioactive compounds, predominately containing flavonoids, chalcones, and triterpenoids (Ye et al., 2004; Wang et al., 2016), and the extract of *C. operculatus* flower buds exerts various pharmacological activities *in vitro* and *in vivo*, including anti-hyperglycemic and cardio tonic effects (Mai and Chuyen, 2007; Woo et al., 2002; Mai et al., 2010;Dung et al., 2008). However, the protective effect of the extract of *C. operculatus* flower buds against LPS-induced endotoxic shock remains unclear. The aim of the present study was to investigate the anti-inflammatory effects of ethanol extract of *C. operculatus* flower buds (ECO) and its major constituent 2′,4′-dihydroxy-6′-methoxy-3′,5′-dimethylchalcone (DMC) in macrophages and in an experimental sepsis mouse model, and their underlying mechanisms. The results of this study showed that ECO and DMC inhibited LPS-induced inflammatory response *in vitro* and *in vivo* by activating the Nrf2/HO-1 pathway in macrophages.

2. Materials and methods

2.1. Cell culture and isolation of bone marrow-derived macrophages

RAW264.7 cells were purchased from the American Type Culture Collection (Manssas, VA, USA) and cultivated in Dulbecco's modified Eagle medium (DMEM) supplemented with 10% heat-inactivated fetal bovine serum (FBS; Cambrex, Charles City, IA, USA) in a humidified 5% CO_2 containing atmosphere at 37 °C. Bone marrow-derived macrophages (BMMs) were prepared as previously described (Tran et al., 2018). In brief, bone marrow cells were isolated from femurs and tibias of 6 week-old male ICR mice and incubated overnight with α-MEM (Hyclone, Logan, UT, USA) containing 10% FBS, 100 U/mL penicillin, 100 μg/mL streptomycin, and 10 ng/mL M-CSF (Prospec, East Brunswick, NJ, USA). Floating cells were collected and cultured for 3 days in the presence of 30 ng/mL M-CSF. Cells adhering to the bottom of the culture dish were classified as BMMs and used for further experiments.

2.2. Materials

SB203580, SP600125, and U0126 were purchased from Calbiochem (San Diego, CA, USA). Tin protoporphyrin IX (SnPP) and copper protoporphyrin IX (CuPP) were obtained from Porphyrin Products Inc. (Logan, UT, USA). N-acetyl-L-cysteine (NAC) and an anti-α-tubulin antibody were purchased from Sigma (St. Louis, MO, USA). Antibodies against HO-1, cyclooxygenase-1 (COX-2), Nrf2, and glyceraldehyde 3-phosphate dehydrogenase (GAPDH) were purchased from Santa Cruz Biotechnology (Santa Cruz, CA, USA). Antibodies against phospho-AKT, AKT, phospho-p38, p38, phospho-ERK1/2, ERK1/2, phospho-JNK, JNK, and poly ADP-ribose polymerase (PARP) were obtained from Cell Signaling Technology (Danvers, MA, USA). Antibody against inducible nitric oxide synthase (iNOS) was obtained from EMD Millipore (Billerica, MA, USA). ELISA kits for IL-6, IL-1β and TNF-α were supplied by R&D systems (Minneapolis, MN, USA).

2.3. Preparation of ethanol extract of C. operculatus flower buds and isolation of DMC

The dried flower buds of *C. operculatus* were obtained from National Institute of Medicinal Materials (Ha Noi, Viet Nam) in September 2017 and identified by Professor Byung Sun-Min (College of Pharmacy, Daegu Catholic University, Gyeongbuk, Republic of Korea). The voucher specimen (CUD-3181) was deposited at the Herbarium of the College of Pharmacy, Daegu Catholic University. The dried flower buds of *C. operculatus* (50.0 g) were extracted three times (3 h × 500 mL) with ethanol at room temperature. The extract was then filtered and concentrated by a rotary evaporator and finally dried by a freeze drier to obtain ECO (5.5 g). DMC was isolated from the buds of *C. operculatus* as previously described (Ye et al., 2004). DMC was obtained as orange yellow needles and showed an $[M]^+$ peak at *m/z* 321.1 by electron ionization-mass spectrometry (calculated for $C_{18}H_{16}O_5$).

2.4. Quantification of DMC in ECO

To quantify DMC in ECO, the external standard method was applied. High performance liquid chromatography (HPLC) analysis was performed using HPLC Waters 2695 system, on Sunfire® C18 column (4.6 × 150 mm, 5 μm). Mobile phase consisted of A (acetonitrile) and B (0.1% TFA in water). The elution program was isocratic at 60% (A) and 40% (B) for 20 min, at 1 mL/min flow rate. The injection volume was 10 μL (2 mg/mL) and the peak area of DMC was determined at a wavelength of 330 nm. The peak areas were used to calculate the concentration of DMC in ECO.

2.5. Measurement of NO, IL-1β, IL-6, TNF-α, and cell viability

BMMs (2×10^5 cells/well) or RAW264.7 cells (1×10^5 cells/well) were seeded into 24-well plates. The cells were then treated with various concentrations of ECO or DMC for 30 min followed by incubation for another 24 h in the presence or absence of LPS (1 μg/mL). For certain experiments, SnPP or CuPP was added to the plates together with ECO or DMC. Total NO metabolite concentration in the culture supernatant was measured using the Griess reaction. The concentrations of TNF-α, IL-1β, and IL-6 in the culture supernatant were quantified using ELISA assay kits according to the manufacturer's protocol. The MTT [3-(4,5-dimethylthiazolyl-2)-2,5-diphenyltetrazolium bromide]-based colorimetric assay was used to determine cell viability.

2.6. Determination of ROS level

Cells were loaded for 30 min with 2′,7′-dichlorofluorescin diacetate (DCF-DA) in the dark, followed by incubation with DMC for 30 min at 37 °C in the dark. Fluorescence was analyzed at an excitation wavelength of 480 nm and an emission wavelength of 535 nm using a Synergy MX Multi-Mode Microplate Reader (BioTek Instruments, Winooski, VT, USA). The intracellular ROS levels were expressed as DCF-DA fluorescence intensity.

2.7. Western blot analysis

Whole cell lysates were prepared using a cell lysis buffer [50 mM Tris-HCl (pH 7.5), 1% Nonidet P-40, 1 mM EDTA, 1 mM phenylmethylsulfonyl fluoride, 10 μg/mL pepstatin A, 10 μg/mL aprotinin, 2 mM benzamidine, 50 mM NaF, 5 mM sodium orthovanadate, and 150 mM NaCl]. Cytoplasmic and nuclear extracts were prepared using NE-PER Nuclear and Cytoplasmic Extraction Reagent Kit according to the manufacturer's instructions (Thermo Fisher Scientific, Rockford, IL, USA). Equal amounts of proteins were electrophoresed in a sodium dodecyl sulfate-polyacrylamide gel electrophoresis (SDS-PAGE), and the proteins were transferred to a Hybond-P membrane (Amersham Biosciences, Buckinghamshire, UK). Membranes were blocked with 5%

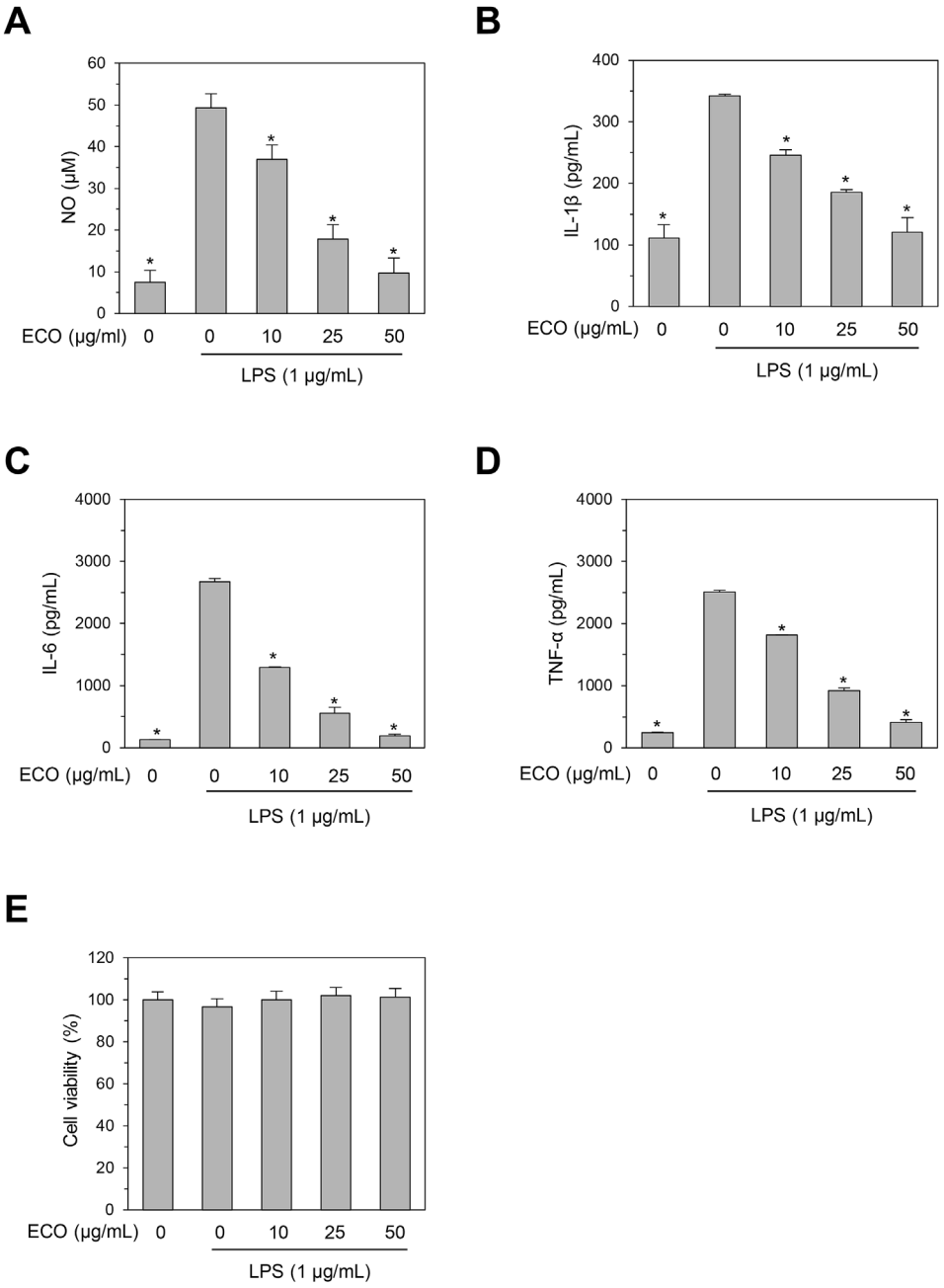

Fig. 1. ECO inhibits the LPS-induced inflammatory response in RAW264.7 cells. (A, B, C, and D) RAW264.7 cells were pretreated with the indicated concentrations of ECO for 30 min, followed by stimulation with LPS (1 μg/mL). After 24 h of incubation, the levels of NO (A), IL-1β (B), IL-6 (C), and TNF-α (D) were measured in the culture supernatants. Data represent mean ± SEM (*, $p < 0.01$ compared with LPS plus vehicle treated control, $n = 5$). E) RAW264.7 cells were treated with the indicated concentrations of ECO for 24 h and cell viability was evaluated using the MTT assay. Data represent mean ± SEM (*, $p < 0.01$ compared with LPS plus vehicle treated control, $n = 5$).

skimmed milk at room temperature for 1 h to block non-specific binding. Proteins were detected by incubation with primary antibodies (1:1,000 dilution) followed by incubation with the appropriate secondary antibody conjugated to horseradish peroxidase (1:2,000 dilution). Signals were visualized using ECL system according to the manufacturer's instructions (Thermo Fisher Scientific).

2.8. Quantitative polymerase chain reaction (qPCR)

The cells were harvested and total RNA was isolated using RNeasy Mini Kits according to the manufacture's instructions (Qiagen, Valencia, CA, USA). One microgram of total RNA was used to synthesize first-strand complimentary DNA using an RT-PCR kit (Invitrogen, Carlsbad, CA, USA). Real-time qPCR amplification was carried out using TOPreal qPCR 2X PreMIX (SYBR Green, Enzynomics. Daejon, Korea) and Rotor-Gene Q real-time PCR cycler (Qiagen). The following primers were used: *IL-6,* 5′-TCC ATC CAG TTG CCT TCT TGG-3' (sense) and 5′-CCA CGA TTT CCC AGA GAA CAT G-3' (antisense); *TNF-α*, 5′-GCT GGC ACC ACT ACT TGG TT-3' (sense) and 5′-AGC AAA AAG CCA CCA AGT GGA GG-3' (antisense); *iNOS*, 5′-GGC AAA CCC AAG GTC TAC GTT-3' (sense) and 5′-TCG CTC AAG TTC AGC TTG GT-3' (antisense); *COX-2*, 5′-TGA GTA CCG CAA ACG CTT CT-3' (sense) and 5′-CTC CCC AAA GAT AGC ATC TGG-3' (antisense); *HO-1*, 5′- CGC AAC AAG CAG AAC CCA-3′ (sense) and 5′- GCG TGC AAG GGA TGA TTT CC-3′ (antisense); *NQO1*, 5′-CGC CTG AGC CCA GAT ATT GT-3' (sense) and 5′-GCA CTC TCT CAA ACC AGC CT-3' (antisense); *GCLC*, 5′-GTC TGA CAC GTA GCC TCG GTA A-3' (sense) and 5′-TGG CCA CTA TCT GCC CAA TT-3' (antisense); and *β-actin*, 5′-GGG AAA TCG TGC GTG ACA TCA AAG-3′ (sense) and 5′-AAC CGC TCG TTG CCA ATA GT-3' (antisense). The optimized real-time PCR conditions were 95 °C for 10 min, followed by 40 cycles of 95 °C for 10 s, 60 °C for 15 s, and 72 °C for 20 s. All reactions were performed in triplicate, and β-actin was used as the internal control. Relative gene expression was quantified using the 2-ΔΔCt method.

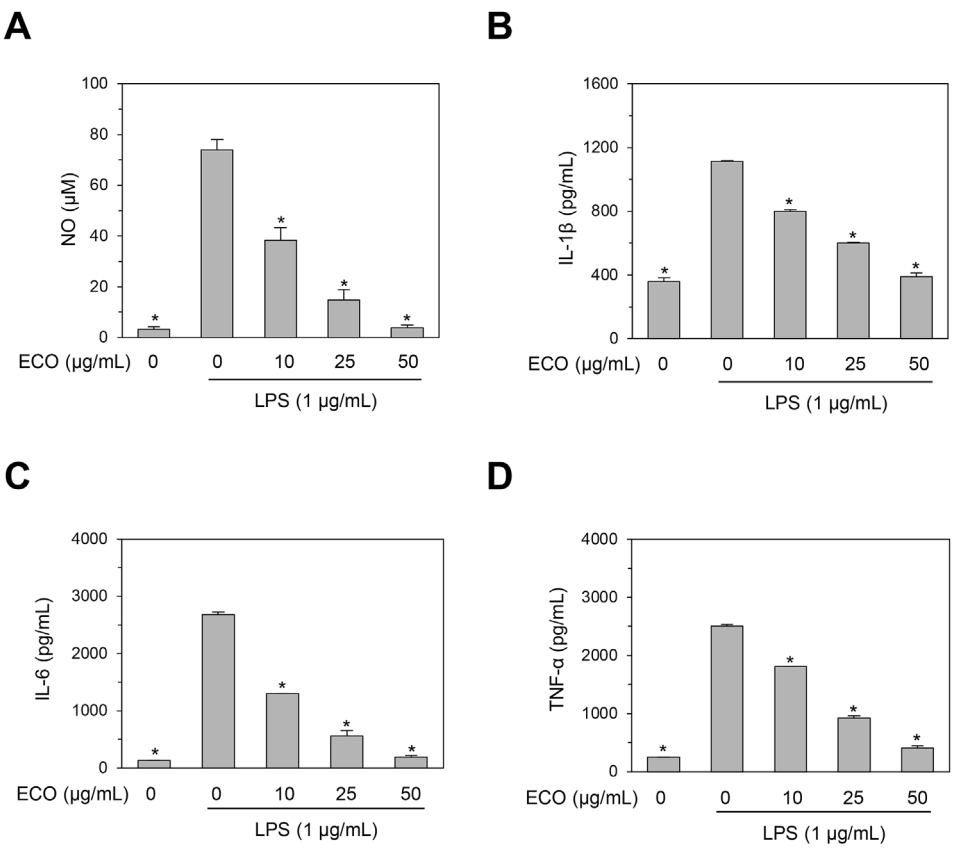

Fig. 2. ECO inhibits the LPS-induced inflammatory response in BMMs. (A, B, C, and D) BMMs were pretreated with the indicated concentrations of ECO for 30 min, followed by stimulation with LPS (1 μg/mL). After 24 h of incubation, the levels of NO (A), IL-1β (B), IL-6 (C), and TNF-α (D) were measured in the culture supernatants. Data represent mean ± SEM (*, $p < 0.01$ compared with LPS plus vehicle treated control, $n = 5$).

2.9. Small interfering RNA, transfection, and NF-κB reporter assay

Nrf2 small interfering RNA (siRNA) and the scrambled control siRNA were obtained from OriGene Technologies (Rockville, MD, USA). Briefly, RAW264.7 cells were plated in 60 mm culture dishes, and then transfected with Nrf2 siRNA or the control siRNA using Fugene HD, according to the instructions of the manufacturer (Promega, Madison, WI, USA). After 48 h, the cells were used for further experiments. Efficiency of Nrf2 knockdown was determined by Western blot analysis. RAW264.7 cells were transfected with pNF-κB-Luc (Stratagene, La Jolla, CA, USA) together with pRL-CMV vector (Promega, Madison, WI, USA) as an internal control using Fugene 6 (Promega). After 24 h, the cells were treated for 30 min with various concentrations of DMC, and then stimulated with LPS. Luciferase activity was determined with Synergy MX Multi-Mode Microplate Reader (BioTek, Instruments, Winooski, VT, USA) by measuring light emission for 10 s. The results were normalized to the activity of *renilla*.

2.10. Immunofluorescence and confocal microscopy

Cells were rinsed once in PBS, fixed in fresh 4% paraformaldehyde for 20 min at room temperature, and permeabilized in 0.5% TritonX-100 and the blocking was performed with PBS containing 1% goat serum. Cells were then incubated with Nrf2 antibody (1:200 dilution) for 1 h. After four washes in PBS, the cells were incubated with Alexa Fluor 546 goat anti-rabbit secondary antibody (1:250 dilution) for 4 h at room temperature, washed, stained with DAPI, and mounted. Confocal images were acquired using an OLYMPUS FV1000 inverted laser scanning confocal microscope equipped with an external argon laser, HeNe laser Green, and HeNe laser Red. Using a UPLSAPO 60X NA1.35 oil immersion objective (OLYMPUS), images were captured at the colony midsection.

2.11. LPS-induced septic shock and histological assessment

All animal studies were conducted in accordance with procedures approved by the Institutional Animal Care and Use Committee (IACUC) of Kangwon National University (IACUC approval No. KW-180903-3). Five-week-old male ICR mice (DBL, Emseong, Chungbuk, Korea) weighing between 20 and 23 g were used for this study. The mice (five mice per group) were orally administrated with various concentrations of ECO (0, 100, and 200 mg/kg body weight) dissolved in corn oil or the control vehicle (corn oil) or injected intraperitoneally with DMC (0, 50, 100 mg/kg) dissolved in dimethyl sulfoxide:chremophore-EL:PBS (1:1:8 by volume) 1 h before LPS (*Escherichia coli* 0111:B4; Sigma-Aldrich, 20 mg/kg body weight) injection. To determine the survival rate, mortality was monitored for 6.5 days after injecting LPS, after which no further loss of mice occurred. To determine the levels of TNF-α, IL-1β, and IL-6 in serum, the mice were sacrificed 4 h after LPS injection and their blood was collected via cardiac puncture. The serum levels of TNF-α, IL-1β, and IL-6 were quantified using ELISA assay kits, according to the manufacturer's protocol. For histological analysis of liver and lung, the mice were sacrificed 20 h after LPS injection, and liver and lung tissues were collected to be fixed with 4% paraformaldehyde. After 24 h, the tissue samples were cryo-protected in 30% sucrose at 4 °C, and subsequently frozen in OCT compound (Leica Biosystems, Richmond, USA). They were then cut into 10 μm sections, and stained with hematoxylin–eosin Y (Sigma-Aldrich). Images were taken using a model H550L microscope (Nikon Corporation, Tokyo, Japan) in randomly selected fields (200× magnification).

2.12. Statistical analysis

Data were expressed as the mean ± standard error of mean (SEM). Statistical significance was assessed by one-way analysis of variance and Turkey test to examine the differences between the two groups using SPSS (version 14.0; SPNN Inc., Chicago, IL, USA). *P* values less

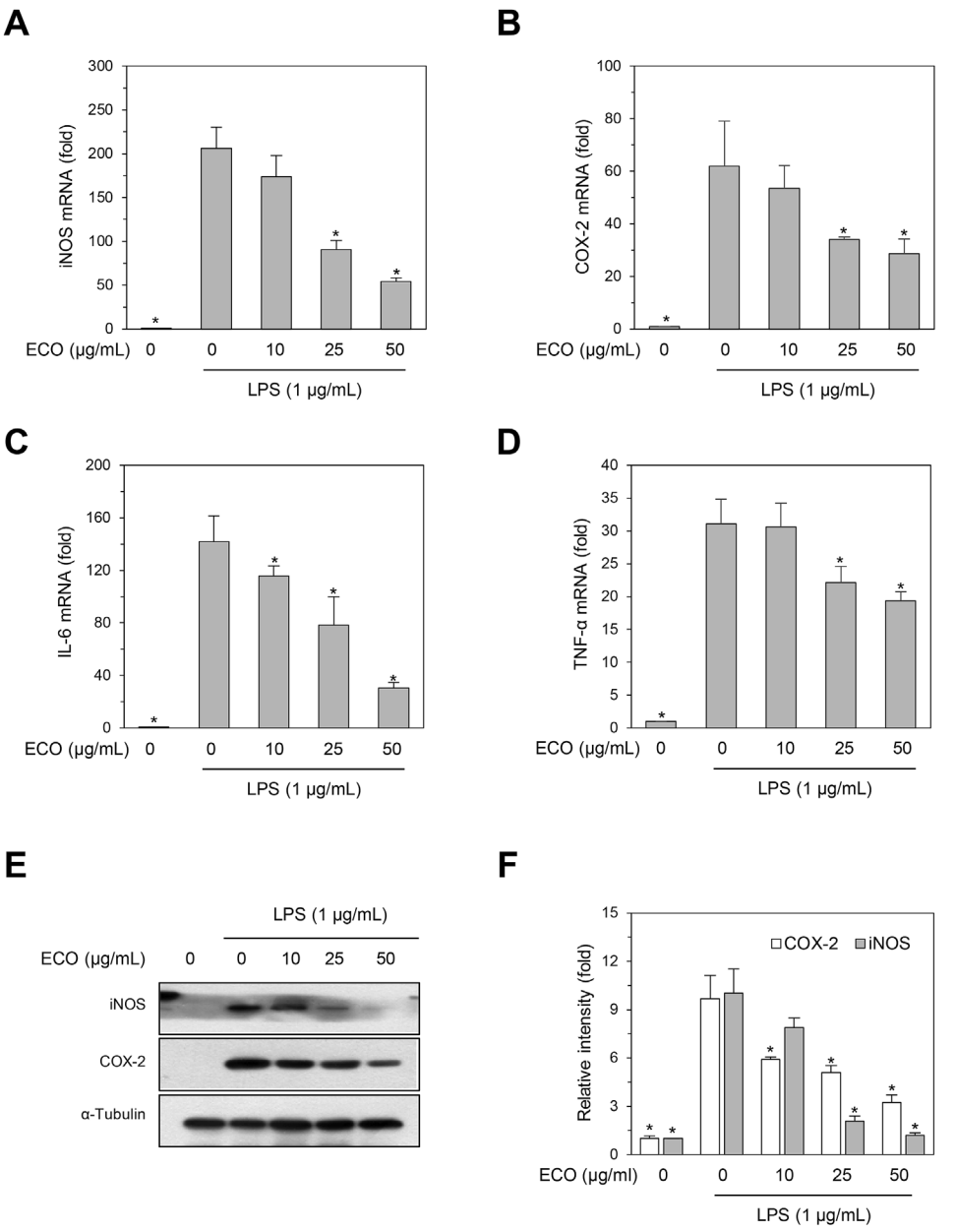

Fig. 3. ECO inhibits the LPS-induced expression of pro-inflammatory mediators. (A, B, C, and D) RAW264.7 cells were pretreated for 30 min with the indicated concentrations of ECO, followed by stimulation with LPS (1 μg/mL) for 8 h. Subsequently, total RNA was prepared, and iNOS (A), COX-2 (B), IL-6 (C), and TNF-α (D) mRNA expression levels were measured by real-time qPCR. Data represent mean ± SEM (*, $p < 0.01$ compared with LPS plus vehicle treated control, $n = 6$). (E) RAW264.7 cells were pretreated for 30 min with the indicated concentrations of ECO, followed by stimulation with LPS (1 μg/mL) for 24 h. Subsequently, total lysates were prepared and iNOS and COX-2 expression levels were measured by Western blot analysis. Representative images are shown. (F) Densitometric analyses of iNOS and COX-2 expressions (normalized to α-tubulin) expressed as the mean ± SEM of three independent experiments (*, $p < 0.01$ compared with vehicle-treated control).

than 0.05 was considered to be statistically significant.

3. Results

3.1. ECO inhibits LPS-induced production of NO, IL-1β, IL-6, and TNF-α in RAW264.7 cells and BMMs

We determined the effects of ECO on LPS-induced production of inflammatory mediators in RAW264.7 cells (Fig. 1A–D). Upon LPS stimulation, the levels of NO, IL-1β, IL-6, and TNF-α in the culture supernatant were significantly increased. However, pretreatment of the RAW264.7 cells with ECO inhibited the LPS-induced production of NO, IL-1β, IL-6, and TNF-α in a concentration-dependent manner, with IC_{50} values of 15.7 ± 0.8, 13.5 ± 0.5, 13.2 ± 0.7, and 15.6 ± 1.2 μg/mL, respectively. However, treatment of RAW264.7 cells with up to 50 μg/mL ECO did not significantly decrease the cell viability (Fig. 1D). We next investigated the anti-inflammatory effect of ECO in primary cultures of BMMs. Similar to the effects in RAW264.7 cells, ECO inhibited the LPS-induced production of NO, IL-1β, IL-6, and TNF-α in a concentration-dependent manner with IC_{50} values of 10.2 ± 0.5, 12.1 ± 0.8, 9.5 ± 0.7, and 12.8 ± 0.6 μg/mL, respectively (Fig. 2A–D). These results suggested that ECO inhibited the LPS-induced inflammatory response in macrophages without affecting cell viability.

3.2. ECO downregulates LPS-induced expression of pro-inflammatory mediators

Next, we determined whether ECO suppresses LPS-induced iNOS, COX-2, IL-6, and TNF-α mRNA expression using real-time qPCR analysis. Treatment of RAW264.7 cells with ECO decreased the LPS-induced expression levels of iNOS, COX-2, IL-6, and TNF-α mRNA in a concentration-dependent manner (Fig. 3A–D). Consistent with this result, Western blot analysis also revealed that ECO suppressed LPS-induced iNOS and COX-2 protein expression in a concentration-dependent manner (Fig. 3E and F). These results suggested that ECO suppressed the LPS-induced expression of inflammatory mediators at the transcriptional level.

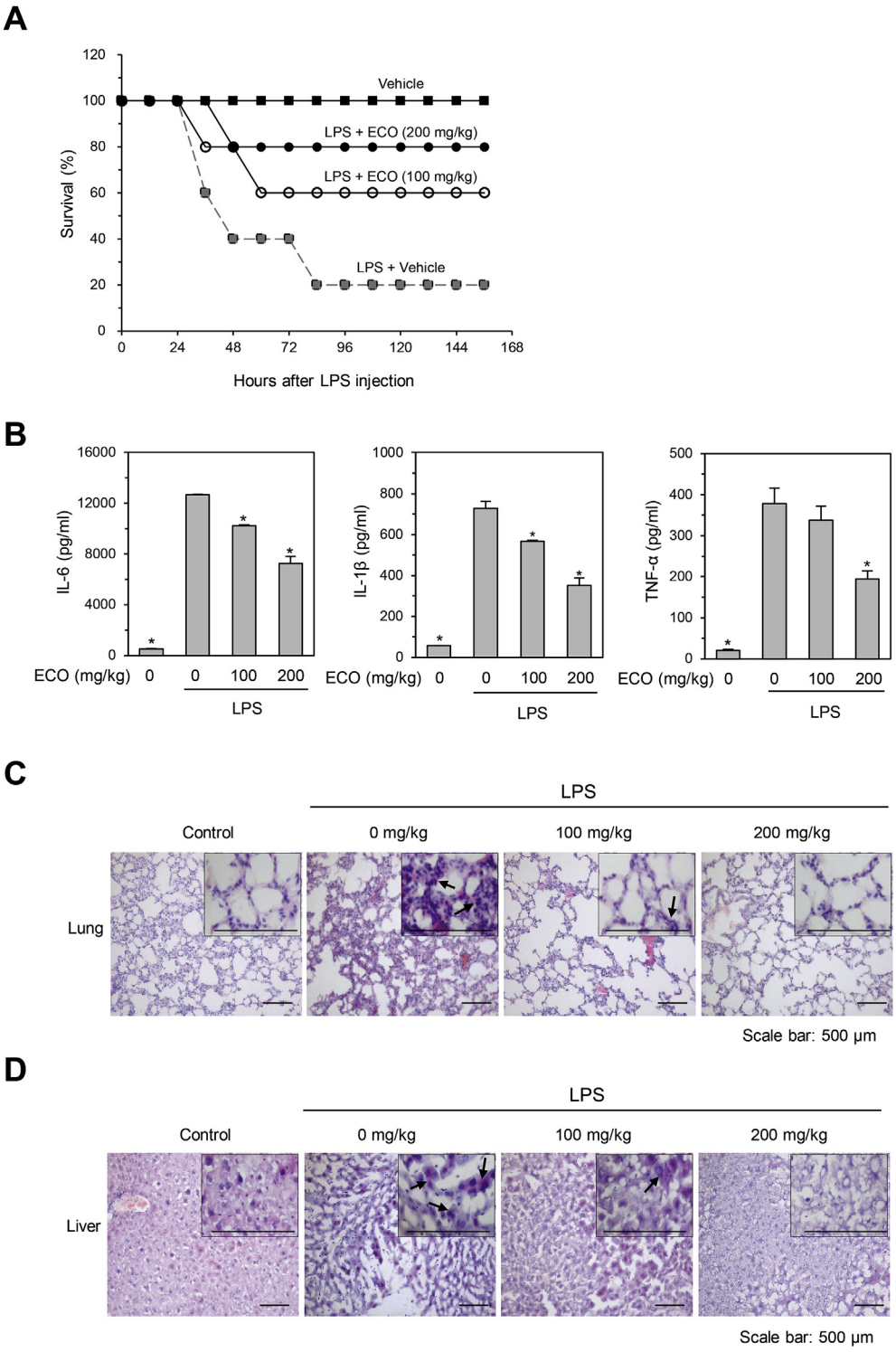

Fig. 4. ECO protects the mice from LPS-induced endotoxic shock. Mice were challenged with LPS after oral administration of ECO (100 or 200 mg/kg) or control vehicle. (A) Survival was monitored during 6.5 days after LPS injection. (B) Animals were sacrificed 4 h after LPS injection and the blood was collected by cardiac puncture. Serum levels of IL-1β, IL-6, and TNF-α were measured. Data represent mean ± SEM (*, $P < 0.01$ compared with LPS plus vehicle treated control, $n = 4$. (C and D) Animals were sacrificed 20 h after LPS injection and tissues of the lung (C) and liver (D) were collected of hematoxylin–eosin (H&E) staining. The images show H&E staining from lung and liver tissue sections from the indicated group. The infiltration of inflammatory cells are indicated by black arrows.

3.3. ECO protects ICR mice from LPS-induced mortality and tissue damage

To evaluate the anti-inflammatory effect of ECO *in vivo*, we employed the classical sepsis models induced by LPS. Mice were administrated with either ECO or vehicle, and were intraperitoneally challenged 1 h later with 20 mg/kg LPS to induce experimental sepsis. LPS-treated mice began to die at 36 h and four of five mice died within 4 days. In contrast, the oral administration of 100–200 mg/kg of ECO resulted in the survival of 60%–80% of the mice on the final day, respectively (Fig. 4A). The serum levels of IL-1β, IL-6 and TNF-α were also significantly increased after LPS administration; however, the oral administration of ECO suppressed LPS-induced increase in serum levels of these pro-inflammatory mediators in a dose-dependent manner (Fig. 4B). Histological analysis revealed that lung tissue of LPS group exhibited several inflammatory changes such as thickening of the alveolar wall and alveolar congestion; however, the administration of ECO markedly alleviated the swelling of alveolar wall and declined alveolar congestion in LPS-challenged mice (Fig. 4C) in LPS-challenged mice (Fig. 4C). Histological damage was observed in the liver of the LPS group. It was characterized by hepatic disarray, hepatic lobule

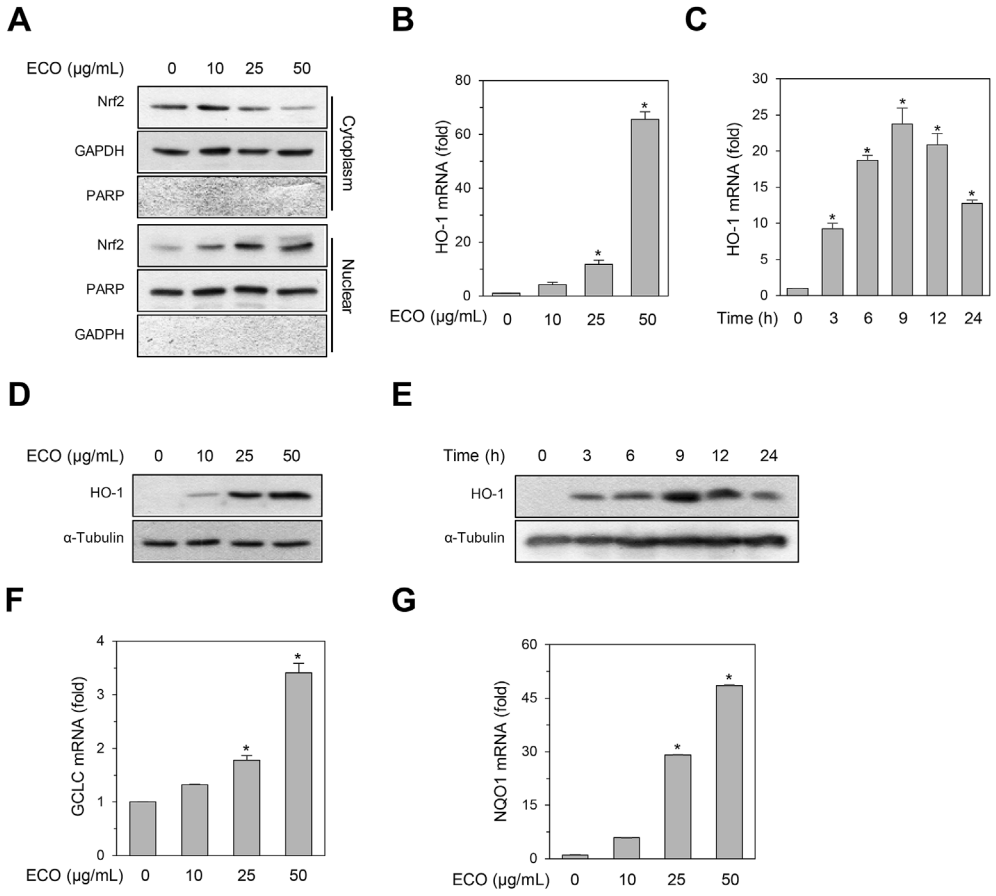

Fig. 5. ECO activates Nrf2. (A) RAW264.7 cells were treated for 2 h with the indicated concentrations of ECO. Nuclear and cytosolic extracts were subjected to Western blot analysis to determine Nrf2 levels. PARP was used as a nuclear marker and GAPDH was used as a cytosolic protein marker. Representative images are shown. (B and C) RAW264.7 cells were treated with the indicated concentrations of ECO for 6 h (B) or 50 μg/mL ECO for the indicated periods of time (C). Subsequently, total RNA was prepared, and HO-1 mRNA expression levels were determined by real-time qPCR. Data represent mean ± SEM (*, $p < 0.01$ compared with vehicle-treated control, $n = 6$). (D and E) RAW264.7 cells were treated for 9 h with the indicated concentrations of ECO (D) or 50 μg/mL ECO for the indicated periods of time (E). Total cell lysates were prepared and HO-1 expression levels were determined by Western blot analysis. (F and G) RAW264.7 cells were treated for 6 h with the indicated concentrations of ECO. Subsequently, total RNA was prepared and NQO1 (G) and GCLC (H) mRNA expression levels were determined by real-time qPCR. Data represent mean ± SEM (*, $p < 0.01$ compared with vehicle-treated control, $n = 5$).

distortion, and infiltration of inflammatory cells. These changes were significantly inhibited by oral administration of 200 mg/kg of ECO (Fig. 4D). These results suggested that ECO protected mice from the LPS-induced tissue damage and mortality.

3.4. ECO activates Nrf2/HO-1 pathway

To investigate the anti-inflammatory mechanisms of ECO, we further determined whether ECO activates Nrf2 in RAW264.7 cells. Treatment of RAW264.7 cells with ECO increased nuclear accumulation of Nrf2 (Fig. 5A). To further confirm ECO-induced activation of Nrf2, we determined whether ECO induces the expression of Nrf2 target genes, including HO-1, NQO1, and GCLC in RAW264.7 cells. Treatment of RAW264.7 cells with ECO increased HO-1 mRNA and protein levels in a time- and concentration-dependent manner (Fig. 5B–E). ECO also increased the expression level of NQO1, and GCLC mRNA in RAW264.7 cells (Fig. 5F and G), suggesting that ECO activated Nrf2 in RAW264.7 cells.

3.5. Inhibition of HO-1 reverses anti-inflammatory activity of ECO

Since HO-1 is considered as a major anti-inflammatory enzyme that is regulated by Nrf2 activation (Paine et al., 2010; Abraham and Kappas, 2008; Motterlini and Foresti, 2014), we examined whether the ECO-mediated induction of HO-1 was involved in the anti-inflammatory effects of ECO. SnPP, a specific HO-1 inhibitor, significantly reversed the ECO-mediated suppression of NO, IL-1β, IL-6, and TNF-α production in LPS-stimulated BMMs, however, CuPP, a negative inhibitor, did not reverse the anti-inflammatory effects of ECO (Fig. 6A–D). These results suggested that ECO-mediated induction of HO-1 via Nrf2 activation might mediate the anti-inflammatory effects of ECO in macrophages.

3.6. DMC is the major constituent of ECO and exerts anti-inflammatory activity by activating Nfr2/HO-1 pathway

To quantify the content of DMC in ECO, we performed HPLC analysis using the established HPLC protocol. DMC constituted 37.9% of ECO (Supplementary data), indicating that DMC is the major constituent of ECO. We next determined the effects of DMC on LPS-induced inflammatory responses *in vitro* and *in vivo*. Pretreatment of the RAW264.7 cells with DMC inhibited the LPS-induced production of NO, IL-1β, IL-6, and TNF-α in a concentration-dependent manner, with IC_{50} values of 5.2 ± 0.7, 14.5 ± 0.9, 10.6 ± 0.8, and 28.6 ± 1.2 μM, respectively (Fig. 7A–D). Moreover, intraperitoneal administration of 50–100 mg/kg of DMC resulted in the survival of 60%–80% of the mice on the final day, respectively (Fig. 7E). These results suggested that DMC also suppressed LPS-induced inflammatory response *in vitro* and *in vivo*.

We next determined whether DMC activates Nrf2 in RAW264.7 cells, in the manner similar as that of ECO. Treatment of RAW264.7 cells with DMC increased nuclear accumulation of Nrf2 and the expression levels of Nrf2 target genes, such as HO-1, NQO1, and GCLC in RAW264.7 cells (Fig. 8A–D). Moreover, Nrf2 knockdown by siRNA significantly suppressed DMC-induced HO-1 expression (Fig. 8E), and reversed DMC-mediated suppression of iNOS, IL-6, and TNF-α expression in LPS-stimulated RAW264.7 cells (Fig. 8F–H), suggesting that DMC, the major constituent of ECO, also exerted anti-inflammatory effects by activating Nrf2/HO-1 pathway in macrophages.

3.7. DMC activates Nrf2 via ROS-dependent p38 MAPK pathway

Treatment of RAW264.7 cells with DMC increased the intracellular ROS level in a concentration-dependent manner (Fig. 9A). However, treatment with the antioxidant, NAC, significantly suppressed DMC-

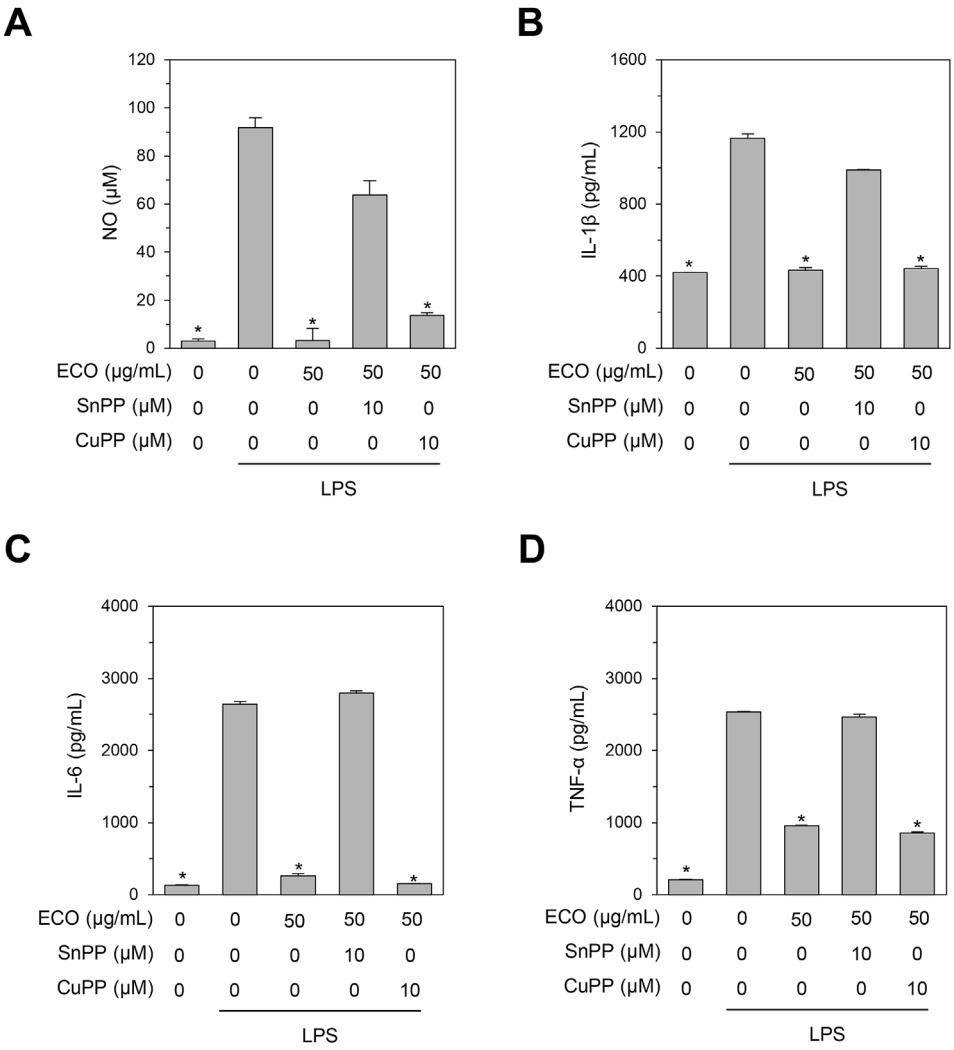

Fig. 6. Inhibition of HO-1 reverses the anti-inflammatory effects of ECO in BMMs. (A, B, C, and D) BMMs were pretreated with ECO (50 μg/mL) in the presence of SnPP or CuPP for 30 min, followed by stimulation with LPS (1 μg/mL) for 24 h. The levels of NO (A), IL-1β (B), IL-6 (C), and TNF-α (D) were measured in culture supernatants. Data represent mean ± SEM (*, $p < 0.01$ compared with LPS plus vehicle treated control, $n = 5$).

induced intracellular ROS production, suggesting that DMC may induce intracellular ROS production. As ROS mediate activation of various kinases, including MAPKs (Ray et al., 2012), we determined whether DMC induces the activation of MAPKs. Treatment of RAW264.7 cells with DMC enhanced the phosphorylation levels of p38 and JNK MAPKs but not ERK1/2 in a time-dependent manner (Fig. 9B). We next investigated whether inhibition of MAPKs affected DMC-mediated Nrf2 activation. Co-treatment of RAW264.7 cells with SP600125 (JNK inhibitor) or U0126 (MEK inhibitor) failed to inhibit DMC-induced Nrf2 nuclear translocation (Fig. 9C). In contrast, SB203580 (p38 inhibitor) significantly blocked ECO-induced nuclear translocation of Nrf2, similar to NAC. The results of real-time qPCR analysis also revealed that SB203580 or NAC significantly decreased DMC-induced HO-1, NQO1, and GCLC mRNA expression levels (Fig. 9D–F). Overall, these results suggested that DMC activated Nrf2 via a ROS-dependent p38 pathway in macrophages.

3.8. DMC inhibits LPS-induced activation of NF-κB and MAPKs

Activating Nrf2 suppresses activation of NF-κB (Li et al., 2008; Cuadrado et al., 2014). Thus, we examined whether DMC suppressed LPS-induced activation of NF-κB and MAPKs. DMC inhibited LPS-induced degradation and resynthesis of IκBα protein, and expression of an NF-κB reporter gene construct (Fig. 10A and B). We also found that pretreating RAW264.7 cells with DMC significantly inhibited LPS-induced phosphorylation ERK, JNK, and p38 MAPK (Fig. 10C).

4. Discussion

C. operculatus has been used as a Vietnamese folk medicine since ancient time. Its buds and leaves were traditionally used to treat fever associated with common cold, bacillary dysentery and gastric inflammation. The dried flower buds of *C. operculatus* are commonly used as an important ingredient in herbal tea and herbal products in tropical countries, especially in Vietnam under the name 'Nu Voi'. In the present study, we demonstrated the protective effect of ECO on LPS-induced inflammatory response and the potential role of the Nrf2/HO-1 pathway in the anti-inflammatory activity of ECO. ECO inhibited LPS-induced inflammatory responses in macrophages, and protected the mice from LPS-induced endotoxic shock and tissue damages. We also showed that ECO and its major constituent DMC activated Nrf2 and induced the expression of Nrf2 target genes, such as HO-1, NQO1, and GCLC, via a ROS-dependent p38 MAPK pathway. Induction of the Nrf2/HO-1 pathway was correlated with suppression of NO, IL-1β, IL-6, and TNF-α expression in LPS-activated macrophages. This is the first report showing that ECO and its major constituent, DMC, may be potential Nrf2 activators in macrophages that suppress the LPS-induced inflammatory response *in vitro* and endotoxic shock *in vivo*. Thus, our

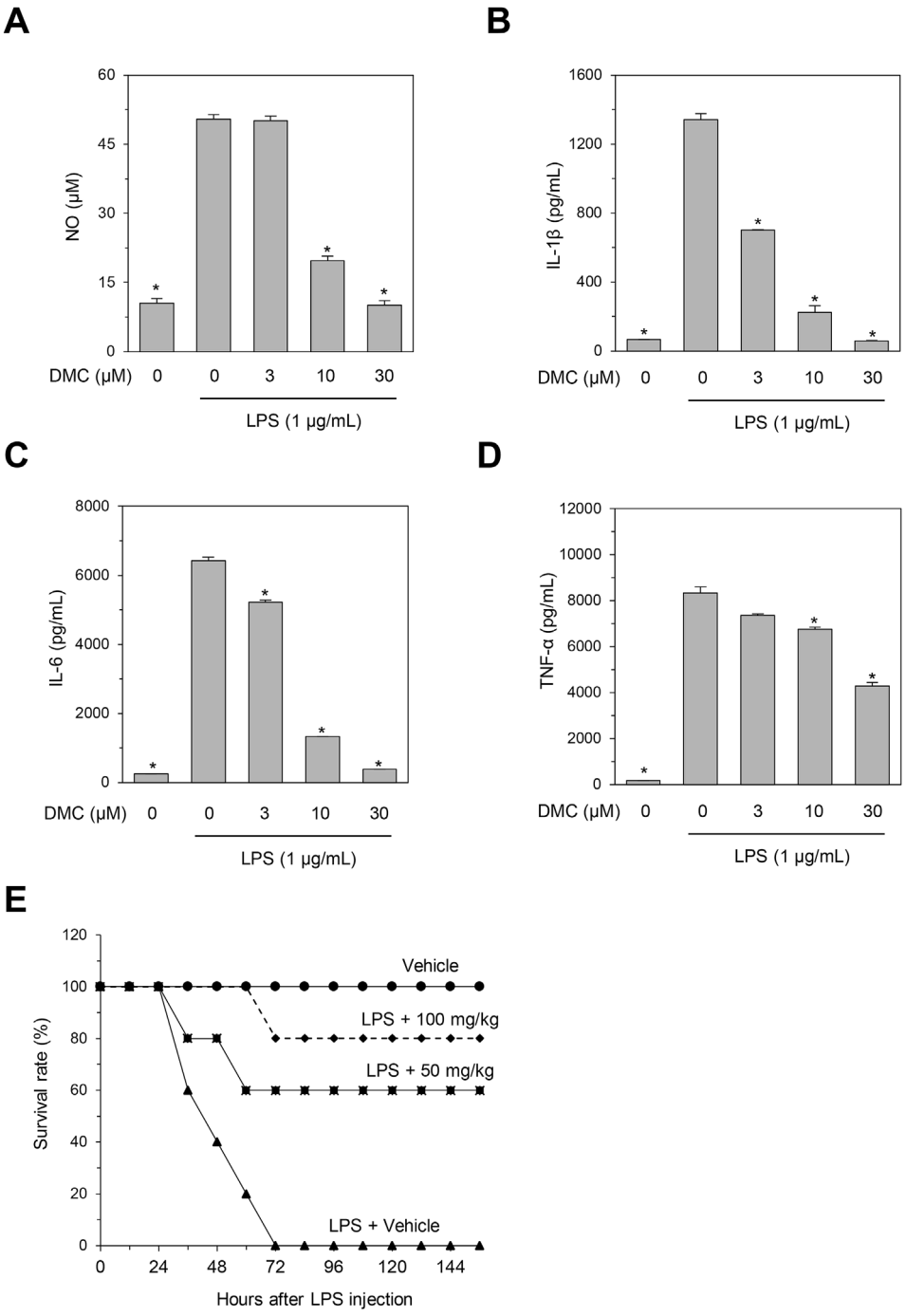

Fig. 7. DMC inhibits the LPS-induced inflammatory response in BMMs and protects the mice from LPS-induced mortality. (A, B, C, and D) BMMs were pretreated with the indicated concentrations of DMC for 30 min, followed by stimulation with LPS (1 μg/mL). After 24 h of incubation, the amounts of NO (A), IL-1β (B), IL-6 (C), and TNF-α (D) were measured in the culture supernatants. Data represent mean ± SEM (*, $p < 0.01$ compared with LPS plus vehicle treated control, $n = 5$). (E) Mice were challenged with LPS after a pre-injection of DMC (50 or 100 mg/kg) or control vehicle. (A) Survival was monitored during 6.5 days after LPS injection.

results provide a pharmacological basis for the medicinal use of the flower buds of *C. operculatus* in inflammatory diseases.

Numerous studies have demonstrated that activation of Nrf2/HO-1 pathway efficiently represses inflammatory responses by inhibiting the expression of many pro-inflammatory mediators. Several phytochemicals, such as resveratrol, curcumin, and sappanone A exert anti-inflammatory effects via activation of Nfr2/HO-1 pathway in different types of cells (Lee et al., 2015; Abuarqoub et al., 2006; Juan et al., 2004; Chen et al., 2005; Liu et al., 2015; Keum et al., 2006;Yao et al., 2015). In addition, several ethanol extracts from medicinal plants also exert anti-inflammatory effect via activation of Nrf2/HO-1 pathway. For example, the ethanol extract of *Inula helenium* L. attenuates LPS-induced inflammatory responses and protects the mice from LPS-induced septic shock via activating Nrf2/HO-1 pathway (Park et al., 2013). In the present study, we showed that ECO activates the Nfr2/HO-1 pathway in macrophages, and suppressed the LPS-induced inflammatory responses *in vitro* and *in vivo*. Thus, ECO-induced activation of Nrf2/HO-1 pathway is at least partially responsible for the anti-inflammatory effects of ECO.

Several anti-inflammatory compounds including chalcones and triterpenoids have been isolated from *C. operculatus* (Wang et al., 2016; Kim et al., 2010). DMC is the major constituent of *C. operculatus* flower

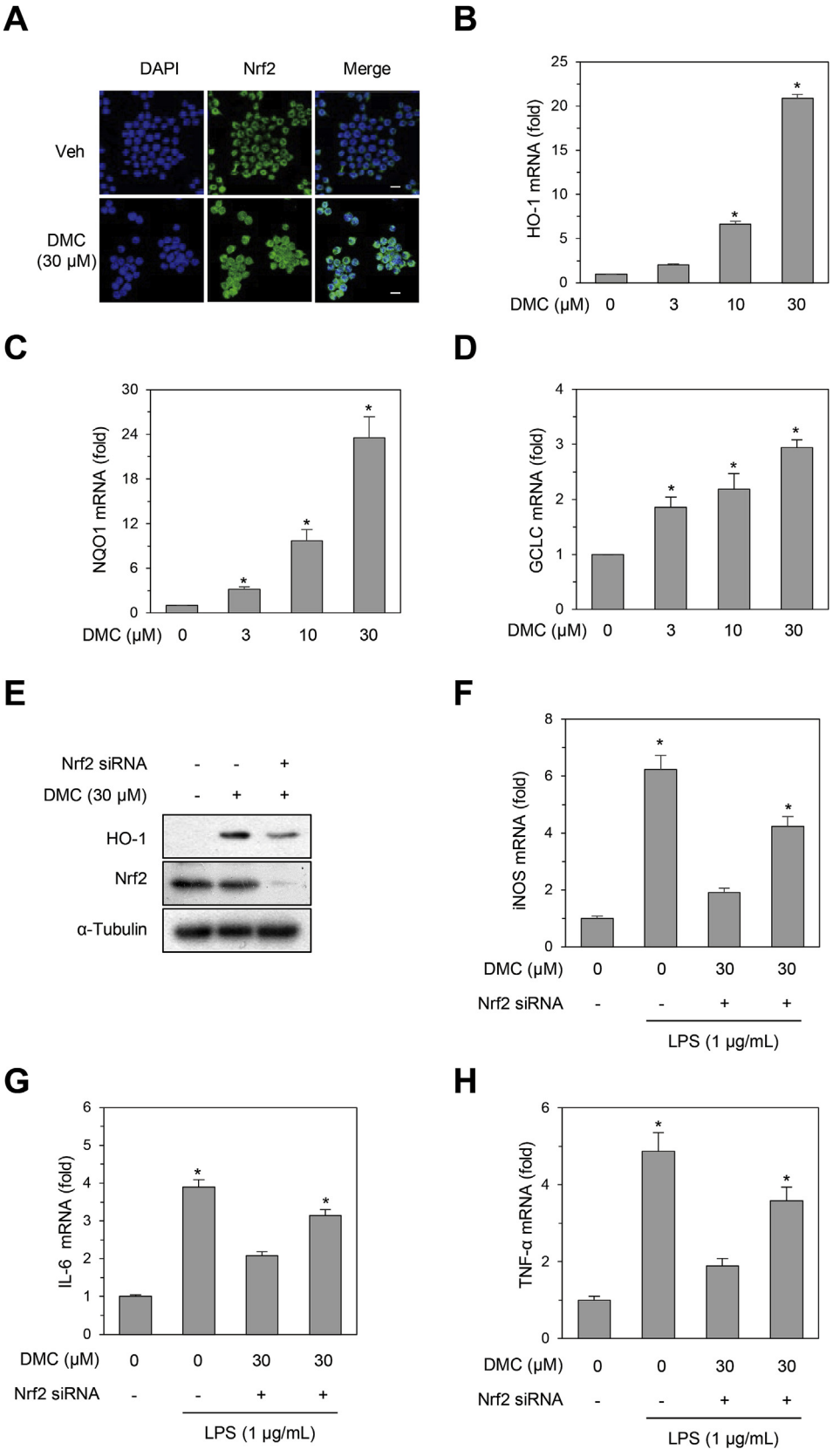

Fig. 8. DMC inhibits LPS-induced inflammatory response via activation of Nrf2/HO-1 pathway. (A) RAW264.7 cells were incubated for 2 h with DMC. Nrf2 was stained with an anti-Nrf2 antibody and then visualized with a secondary antibody conjugated with Alexa Fluor 546. DAPI was used to stain nuclei. Veh: vehicle. Scale bar: 10 μM. (B, C and D) RAW264.7 cells were treated with the indicated concentrations of DMC for 6 h. Subsequently, total RNA was prepared and HO-1 (B), NQO1 (C), and GCLC (D) mRNA expression levels were determined by real-time qPCR. Data represent mean ± SEM (*, $p < 0.01$ compared with vehicle-treated control, $n = 6$). (E) RAW264.7 cells were transfected with the scrambled control siRNA (Con) or Nrf2-targeted siRNA (Nrf2) for 48 h, followed by the treatment with DMC for 8 h. Total cell lysates were prepared and Western blot analysis was performed with the indicated antibodies. (F, G, and H) RAW264.7 cells were transfected with the scrambled control siRNA (Con) or Nrf2-targeted siRNA (Nrf2) for 48 h and then further incubated for 30 min with vehicle or DMC prior to stimulation with LPS (1 μg/mL) for 24 h. Subsequently, total RNA was prepared and iNOS (F), IL-6 (G), and TNF-α (H) mRNA expression levels were determined by real-time qPCR. Data represent mean ± SEM (*, $p < 0.01$ compared with vehicle-treated control, $n = 6$).

buds and exhibits various pharmacological activities, including anti-tumor (Ye et al., 2005; Wei et al., 2018), hepatoprotective (Yu et al., 2011), anti-diabetic (Hu et al., 2014), anti-viral (Ha et al., 2016), and anti-adipogenic effects (Choi et al., 2016). Although previous studies have shown that DMC attenuated LPS-induced inflammatory response in RAW264.7 cells via inhibition of NF-κB activation (Kim et al., 2010; Yu et al., 2015), the underlying mechanisms of anti-inflammatory properties are poorly understood. In the present study, we showed that

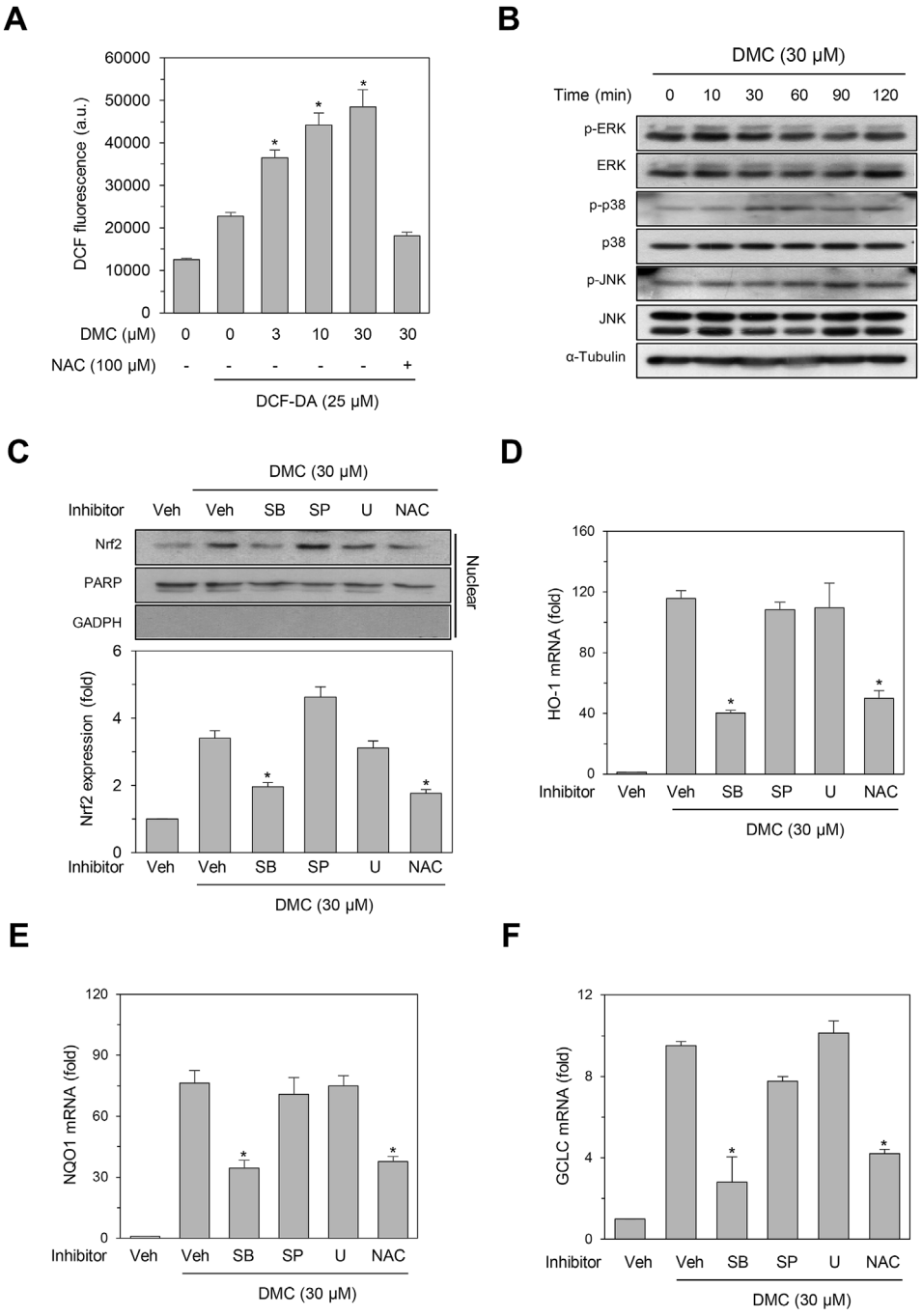

Fig. 9. DMC activates Nrf2 via a ROS-dependent p38 MAPK pathway. (A) RAW264.7 cells were treated with the indicated concentrations of DMC, with or without NAC (100 μM), for 30 min. DCF-DA was used to assess intracellular ROS generation. Data represent mean ± SEM (*, $p < 0.01$ compared with DCF-DA plus vehicle treated control, $n = 6$). (B) RAW264.7 cells were treated for the indicated periods of time with DMC (30 μM), and subsequently whole cell lysates were blotted with the indicated antibodies. (c) RAW264.7 cells were treated for 2 h with DMC (30 μM) alone, or in the presence of SB203580 (SB, 10 μM), SP600125 (SP, 10 μM), U0126 (U, 10 μM), or NAC (100 μM). Nuclear extracts were subjected to Western blot analysis to determine Nrf2 levels. PARP was used as a nuclear marker and GAPDH was used as a cytosolic protein marker. Veh; vehicle. Densitometric analyses of Nfr2 protein expression in nuclear (normalized to PARP) expressed as the mean ± SEM of three independent experiments. *$P < 0.01$ versus DMC plus vehicle treated control. (D, E, and F) RAW264.7 cells were treated for 6 h with DMC (30 μM) alone, or in the presence of SB203580 (SB, 10 μM), SP600125 (SP, 10 μM), U0126 (U, 10 μM), or NAC (100 μM). Subsequently, total RNA was prepared, and the mRNA expression levels of HO-1 (C), NQO1 (D), and GCLC (E) were determined by qPCR. Data are mean ± SEM (*, $p < 0.01$ compared with compared with DMC plus vehicle treated control, $n = 6$). Veh: vehicle.

the content of DMC in ECO is about 37.9%, and both ECO and DMC activated Nrf2/HO-1 pathway. Moreover, inhibition of HO-1 or knockdown of Nrf2 reversed ECO- and DMC-mediated anti-inflammatory effect in macrophages. Thus, MC could potentially be the active constituent responsible for the anti-inflammatory effect of ECO *in vitro* and *in vivo*. It is worth mentioning that DMC inhibits Nrf2 activation and reverses 5-fluorouracil resistance in human hepatocellular carcinoma cells (Wei et al., 2018). DMC suppressed the expression of Nrf2, prevented Nrf2 nuclear translocation, and blocked the binding of Nrf2 to the antioxidant response element (Wei et al., 2018). However, our results clearly showed that DMC induced Nrf2 nuclear translocation and the expression of its target genes in macrophages, indicating that DMC is a potent Nrf2 activator in macrophages. Thus, it is likely that DMC may inhibit or activate Nrf2 in cell type-dependent manner. Further studies will be needed to investigate whether DMC functions as an Nrf2 activator or inhibitor in other types of cells.

Multiple signaling kinases including p38 MAPK have been shown to mediate the activation of Nrf2 (Niture et al., 2014; Jain and Jaiswal, 2007; Shan et al., 2010). ROS can mediate the activation of p38 MAPK by activating apoptosis signal-regulating kinase 1 (ASK1), a member of MAP3K superfamily (Diez et al., 2015; Liu et al., 2000; Hsieh and Papaconstantinou, 2006). Under non-stressed condition, ASK1 remains inactive due to the suppressive effect of reduced thioredoxin (Trx). In response to ROS, Trx is oxidized and is disassociated from ASK1-Trx complex, leading to the activation of ASK1, which, in turn, leads to activation of p38 MAPK signaling pathway (Hsieh and Papaconstantinou, 2006). In the present study, we demonstrated that DMC induced p38 MAPK activation and the potent antioxidant NAC or a specific p38 MAPK inhibitor SB203580 blocked DMC-mediated Nrf2 target gene expression in macrophages, suggesting that DMC induced

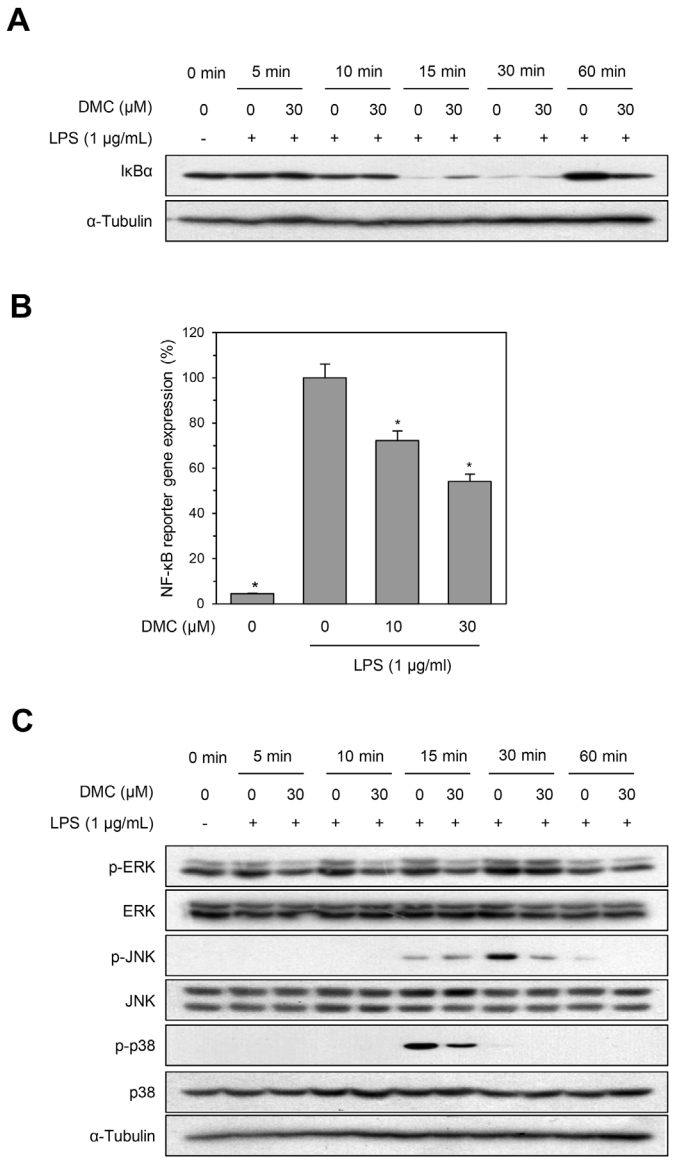

Fig. 10. DMC inhibits LPS-induced activation of NF-κB and MAPKs. (A) RAW264.7 cells were incubated with DMC (30 μM) for 30 min, followed by the stimulation with LPS (1 μg/mL) for the indicated periods of time. Total cell lysates were prepared and then performed Western blot analysis with the indicated antibodies. (B) RAW264.7 cells transfected with a NF-κB-dependent reporter gene construct were incubated with the indicated concentrations of DMC, followed by the stimulation with LPS (1 μg/mL) for 12 h. The cells were lysed, and then luciferase activities were determined. Data are presented as mean ± SEM (*$p < 0.01$ compared with DMC-only treated group, $n = 5$). (C) RAW264.7 cells were incubated with DMC (30 μM) for 30 min, followed by the stimulation with LPS (1 μg/mL) for the indicated periods of time. Total cell lysates were prepared and then performed Western blot analysis with the indicated antibodies.

the activation of Nrf2 via ROS-mediated p38 MAPK activation.

In summary, we demonstrated for the first time that ECO attenuates LPS-induced inflammatory responses *in vitro* and *in vivo* and the ECO-induced activation of the Nrf2/HO-1 pathway in macrophages was associated with anti-inflammatory effects of ECO. Furthermore, our data extended our understanding of the molecular mechanisms underlying the anti-inflammatory effect of ECO and DMC, and provide pharmacological evidence supporting the use of *C. operculatus* in traditional medicine. Our results also suggested that ECO and DMC might be potential Nrf2 activators that could be used for preventing or treating inflammatory diseases.

Conflict of interest

The authors declare no conflict of interest.

Acknowledgments

This work was supported by grants from the National Research Foundation of Korea (NRF-2018R1D1A1B07047187 and NRF-2015M3A9A5031271).

Appendix A. Supplementary data

Supplementary data to this article can be found online at https://doi.org/10.1016/j.fct.2019.04.035.

Transparency document

Transparency document related to this article can be found online at https://doi.org/10.1016/j.fct.2019.04.035

Abbreviations

BMM	bone marrow-derived macrophage
COX-2	cyclooxygenase-2
CuPP	copper protoporphyrin IX
DCF-DA	2′,7′-dichlorofluorescin diacetate
DMC	2′,4′-dihydroxy-6′-methoxy-3′,5′-dimethylchalcone
ECO	ethanol extract of the flower buds of *C. operculatus*
HPLC	high performance liquid chromatography
ELISA	enzyme-linked immunosorbent assay
ERK-1/2	extracellular signal-related kinase-1/2
GCLC	γ-glutamyl cysteine synthetase catalytic subunit
HO-1	heme oxygenase-1
IL	interleukin
iNOS	inducible nitric oxide synthase
JNK	c-Jun NH_2-terminal kinase
LPS	lipopolysaccharide;
MAPK	mitogen-activated protein kinase
M-CSF	macrophage-colony stimulating factor
MD-2	myeloid differentiating factor 2
MTT	3-(4,5-dimethylthiazolyl-2)-2,5-diphenyltetrazolium bromide
MyD88	myeloid differentiation factor-88
NAC	N-acetyl-L-cysteine
NF-κB	nuclear factor kappa B
Nrf2	nuclear factor erythroid 2-related factor 2
NO	nitric oxide
NQO1	NAD(P)H:quinone oxidoreductase 1
PARP	poly ADP-ribose polymerase
qPCR	quantitative polymerase chain reaction
ROS	reactive oxygen species
Tin SnPP	protoporphyrin IX
TLR4	toll-like receptor-4
TNF-α	tumor necrosis factor-α
TRIF	TIR domain-containing adaptor inducing interferon-β.

References

Abraham, N.G., Kappas, A., 2008. Pharmacological and clinical aspects heme oxygenase. Pharm. Rev. 60, 79–127.

Abuarqoub, H., Foresti, R., Green, C., Motterlini, R., 2006. Heme oxygenase-1 mediates the anti-inflammatory actions of 2'-hydroxychalcone in RAW 264.7 murine macrophages. Am. J. Physiol. Cell Physiol. 290, C1092–C1099.

Aderem, A., Ulevitch, R.J., 2000. Toll-like receptors in the induction of the innate immune response. Nature 406, 782–787.

Ahmed, S.M., Luo, L., Namani, A., Wang, X.J., Tang, X., 2017. Nrf2 signaling pathway: pivotal roles in inflammation. Biochim. Biophys. Acta 1863, 585–597.
Akira, S., Takeda, K., 2004. Toll-like receptor signaling. Nat. Rev. Immunol. 4, 499–511.
Benoit, M., Desnues, B., Mege, J.L., 2008. Macrophage polarization in bacterial infections. J. Immunol. 181, 3733–3739.
Bryan, H.K., Olayanju, A., Goldring, C.E., Park, B.K., 2013. The Nrf2 cell defense pathway: keap1-dependent and -independent mechanisms of regulation. Biochem. Pharmacol. 85, 705–717.
Chen, C.Y., Jang, J.H., Li, M.H., Surh, Y.J., 2005. Resveratrol upregulates heme oxygenase-1 expression via activation of NF-E2-related factor 2 in PC12 cells. Biochem. Biophys. Res. Commun. 331, 993–1000.
Choi, J.W., Kim, M., Song, H., Lee, C.S., Oh, W.K., Mook-Jung, I., Chung, S.S., Park, K.S., 2016. DMC (2',4'-dihydroxy-6'-methoxy-3',5'-dimethylchalcone) improves glucose tolerance as a potent AMPK activator. Metabolism 65, 533–542.
Cuadrado, A., Martín-Moldes, Z., Ye, J., Lastres-Becker, I., 2014. Transcription factors NRF2 and NF-κB are coordinated effectors of the Rho family, GTP-binding protein RAC1 during inflammation. J. Biol. Chem. 289, 15244–15258.
Diez, C.E., Miguel, V., Mennerich, D., Kietzmann, T., Perez, P.S., Cadenas, S., Lamas, S., 2015. Antioxidant responses and cellular adjustments to oxidative stress. Redox Biol. 6, 183–197.
Dung, N.T., Kim, J.M., Kang, S.C., 2008. Chemical composition, antimicrobial and antioxidant activities of the essential oil and the ethanol extract of Cleistocalyx operculatus (Roxb.) Merr and Perry buds. Food Chem. Toxicol. 46, 3632–3639.
Ha, T.K., Dao, T.T., Nguyen, N.H., Kim, J., Kim, E., Cho, T.O., Oh, W.K., 2016. Antiviral phenolics from the leaves of *Cleistocalyx operculatus*. Fitoterapia 110, 135–141.
Hsieh, C.C., Papaconstantinou, J., 2006. Thioredoxin-ASK1 complexes levels regulate ROS-mediated p38 MAPK pathway activity in livers of aged and long-lived Snell dwarf mice. FASEB J. 20, 256–268.
Hu, Y.C., Hao, D.M., Zhou, L.X., Zhang, Z., Huang, N., Hoptroff, M., Lu, Y.H., 2014. 2',4'-Dihydroxy-6'-methoxy-3',5'-dimethylchalcone protects the impaired insulin secretion induced by glucotoxicity in pancreatic β-cells. J. Agric. Food Chem. 62, 1602–1608.
Jain, A.K., Jaiswal, A.K., 2007. GSK-3β acts upstream of Fyn kinase in regulation of nuclear export and degradation of NF-E2 related factor 2. J. Biol. Chem. 282, 16502–16510.
Jaramillo, M.C., Zhang, D.D., 2013. The emerging role of the Nrf2-Keap1 signaling pathway in cancer. Genes Dev. 27, 2179–2191.
Juan, S.H., Cheng, T.H., Lin, H.C., Chu, Y.L., Lee, W.S., 2004. Mechanism of concentration-dependent induction of heme oxygenase-1 by resveratrol in human aortic smooth muscle cells. Biochem. Pharmacol. 69, 41–48.
Keum, Y.S., Yu, S., Chang, P.P., Yuan, X., Kim, J.H., Xu, C., Han, J., Agarwal, A., Kong, A.N., 2006. Mechanism of action of sulforaphane: inhibition of p38 mitogen-activated protein kinase isoforms contributing to the induction of antioxidant response element-mediated heme oxygenase-1 in human hepatoma HepG2 cells. Cancer Res. 66, 8804–8813.
Kim, Y.J., Ko, H., Park, J.S., Han, I.H., Amor, E.C., Lee, J.W., Yang, H.O., 2010. Dimethyl cardamonin inhibits lipopolysaccharide-induced inflammatory factors through blocking NF-κB p65 activation. Int. Immunopharmacol. 10, 1127–1134.
Laskin, D.L., Sunil, V.R., Gardner, C.R., Laskin, J.D., 2011. Macrophages and tissue injury: agents of defense or destruction? Annu. Rev. Pharmacol. Toxicol. 51, 267–288.
Lee, S., Choi, S.Y., Choo, Y.Y., Kim, O., Tran, P.T., Dao, C.T., Min, B.S., Lee, J.H., 2015. Sappanone A exhibits anti-inflammatory effects via modulation of Nrf2 and NF-κB. Int. Immunopharmacol. 28, 328–336.
Li, W., Khor, T.O., Xu, C., Shen, G., Jeong, W.S., Yu, S., Kong, A.N., 2008. Activation of Nrf2-antioxidant signaling attenuates NF-κB-inflammatory response and elicits apoptosis. Biochem. Pharmacol. 76, 1485–1489.
Liu, H., Nishitoh, H., Ichijo, H., Kyriakis, J.M., 2000. Activation of apoptosis signal-regulating kinase 1 (ASK1) by tumor necrosis factor receptor-associated factor 2 requires prior dissociation of the ASK1 inhibitor thioredoxin. Mol. Cell Biol. 20, 2198–2208.
Liu, L., Shang, Y., Li, M., Han, X., Wang, J., Wang, J., 2015. Curcumin ameliorates asthmatic airway inflammation by activating nuclear factor-E2-related factor 2/haem oxygenase (HO)-1 signalling pathway. Clin. Exp. Pharmacol. Physiol. 42, 520–529.
Loi, D.T., 1986. Vietnamese Medicinal Plants and Herbs. Hanoi Pub. House Techno. Vietnam, pp. 437–438.
Mai, T.T., Chuyen, N.V., 2007. Anti-hyperglycemic activity of an aqueous extract from flower buds of *Cleistocalyx operculatus* (Roxb.) Merr and Perry. Biosci. Biotechnol. Biochem. 71, 69–76.
Mai, T.T., Yamaguchi, K., Yamanaka, M., Lam, N.T., Otsuka, Y., Chuyen, N.V., 2010. Protective and anticataract effects of the aqueous extract of *Cleistocalyx operculatus* flower buds on beta-cells of streptozotocin-diabetic rats. J. Agric. Food Chem. 8, 4162–4168.
Medzhitov, R., 2008. Origin and physiological roles of inflammation. Nature 454, 428–435.
Moi, P., Chan, K., Asunis, I., Cao, A., Kan, Y.W., 1994. Isolation of NF-E2-related factor 2 (Nrf2), a NF-E2-like basic leucine zipper transcriptional activator that binds to the tandem NF-E2/AP1 repeat of the β-globin locus control region. Proc. Natl. Acad. Sci. U.S.A. 91, 9926–9930.
Motterlini, R., Foresti, R., 2014. Heme oxygenase-1 as a target for drug discovery. Antioxidants Redox Signal. 20, 1810–1826.
Murray, P.J., 2017. Macrophage polarization. Annu. Rev. Physiol. 79, 541–566.
Niture, S.K., Khatri, R., Jaiswal, A.K., 2014. Regulation of Nrf2-an update. Free Radic. Biol. Med. 66, 36–44.
Park, E.J., Kim, Y.M., Park, S.W., Kim, H.J., Lee, J.H., Lee, D.U., Chang, K.C., 2013. Induction of HO-1 through p38 MAPK/Nrf2 signaling pathway by ethanol extract of *Inula helenium* L. reduces inflammation in LPS-activated RAW 264.7 cells and CLP-induced septic mice. Food Chem. Toxicol. 55, 386–395.
Paine, A., Eiz-Vesper, B., Blasczyk, R., Immenschuh, S., 2010. Signaling to heme oxygenase-1 and its anti-inflammatory therapeutic potential. Biochem. Pharmacol. 80, 1895–1903.
Ray, P.D., Huang, B.W., Tsuji, Y., 2012. Reactive oxygen species (ROS) homeostasis and redox regulation in cellular signaling. Cell. Signal. 24, 981–990.
Shan, Y., Wang, X., Wang, W., He, C., Bao, Y., 2010. p38 MAPK plays a distinct role in sulforaphane-induced up-regulation of ARE-dependent enzymes and down-regulation of COX-2 in human bladder cancer cells. Oncol. Rep. 23, 1133–1138.
Tabas, I., Glass, C.K., 2013. Anti-inflammatory therapy in chronic disease: challenges and opportunities. Science 339, 166–172.
Tran, P.L., Tran, P.T., Tran, H.N.K., Lee, S., Kim, O., Min, B.S., Lee, J.H., 2018. A prenylated flavonoid, 10-oxomornigrol F, exhibits anti-inflammatory effects by activating the Nrf2/heme oxygenase-1 pathway in macrophage cells. Int. Immunopharmacol. 55, 165–173 2018.
Wang, C., Wu, P., Tian, S., Xue, J., Xu, L., Li, H., Wei, X., 2016. Bioactive pentacyclic triterpenoids from the leaves of *Cleistocalyx operculatus*. J. Nat. Prod. 79, 2912–2923.
Wei, X., Mo, X., An, F., Ji, X., Lu, Y., 2018. 2',4'-Dihydroxy-6'-methoxy-3',5'-dimethylchalcone, a potent Nrf2/ARE pathway inhibitor, reverses drug resistance by decreasing glutathione synthesis and drug efflux in BEL-7402/5-FU cells. Food Chem. Toxicol. 119, 252–259.
Woo, A.Y., Waye, M.M., Kwan, H.S., Chan, M.C., Chau, C.F., Cheng, C.H., 2002. Inhibition of ATPases by *Cleistocalyx operculatus*. A possible mechanism for the cardiotonic actions of the herb. Vasc. Pharmacol. 38, 163–168.
Yao, J., Zhang, B., Ge, C., Peng, S., Fang, J., 2015. Xanthohumol, a polyphenol chalcone present in hops, activating Nrf2 enzymes to confer protection against oxidative damage in PC12 cells. J. Agric. Food Chem. 63, 1521–1531.
Ye, C.L., Liu, J.W., Wei, D.Z., Lu, Y.H., Qian, F., 2005. *In vivo* antitumor activity by 2',4'-dihydroxy-6'-methoxy-3',5'-dimethylchalcone in a solid human carcinoma xenograft model. Cancer Chemother. Pharmacol. 55, 447–452.
Ye, C.L., Lu, Y.H., Wei, D.Z., 2004. Flavonoids from *Cleistocalyx operculatus*. Phytochemistry 65, 445–447.
Yu, W.G., He, H., Yao, J.Y., Zhu, Y.X., Lu, Y.H., 2015. Dimethyl cardamonin exhibits anti-inflammatory effects via interfering with the PI3K-PDK1-PKCα signaling pathway. Biomol. Ther. (Seoul) 23, 549–556.
Yu, W.G., Qian, J., Lu, Y.H., 2011. Hepatoprotective effects of 2',4'-dihydroxy-6'-methoxy-3',5'-dimethylchalcone on CCl4-induced acute liver injury in mice. J. Agric. Food Chem. 59, 12821–12829.
Zhang, G., Ghosh, S., 2001. Toll-like receptor-mediated NF-κB activation: a phylogenetically conserved paradigm in innate immunity. J. Clin. Investig. 107, 13–19.